L-3-^{11}C-Lactate as a PET Tracer of Myocardial Lactate Metabolism: A Feasibility Study

Pilar Herrero, Carmen S. Dence, Andrew R. Coggan, Zulfia Kisrieva-Ware, Paul Eisenbeis, and Robert J. Gropler

Division of Radiological Sciences, Edward Mallinckrodt Institute of Radiology, Washington University School of Medicine, St. Louis, Missouri

Lactate is a key myocardial energy source. Lactate metabolism is altered in a variety of conditions, such as exercise and diabetes mellitus. However, to our knowledge, noninvasive quantitative measurements of myocardial lactate metabolism have never been performed because of the lack of an adequate radiotracer. In this study we tested L-3-^{11}C-lactate (^{11}C-lactate) as such a tracer. **Methods:** Twenty-three dogs were studied under a wide range of metabolic interventions. ^{11}C-Lactate and ^{13}C-lactate were injected as boluses and PET data were acquired for 1 h. Concomitant arterial and coronary sinus (ART/CS) blood samples were collected to identify ^{13}C-lactate metabolites and to measure fractional myocardial extraction/production of ^{11}C metabolite fractions (^{11}C acidic: $^{11}CO_2$ and ^{11}C-lactate; ^{11}C basic: ^{11}C-labeled amino acids; and ^{11}C neutral: ^{11}C-glucose). Lactate metabolism was quantified using 2 PET approaches: monoexponential clearance analysis (oxidation only) and kinetic modeling of PET ^{11}C-myocardial curves. **Results:** Arterial ^{11}C acidic, neutral, and basic metabolites were identified as primarily ^{11}C-labeled lactate + pyruvate, glucose, and alanine, respectively. Despite a significant contribution of ^{11}C-glucose (23%–45%) and ^{11}C-alanine (<11%) to total arterial ^{11}C activity, both were minimally extracted (+)/produced(−) by the heart (1.7% ± 1.0% and −0.12% ± 0.84%, respectively). Whereas extraction of ^{11}C-lactate correlated nonlinearly with that of unlabeled lactate extraction (r = 0.86, $P < 0.0001$), $^{11}CO_2$ production correlated linearly with extraction of unlabeled lactate (r = 0.89, $P < 0.0001$, slope = 1.20 ± 0.13). In studies with physiologic free fatty acids (FFA) (415 ± 216 nmol/mL), ^{11}C-lactate was highly extracted (32% ± 12%) and oxidized (26% ± 14%), and PET monoexponential clearance and kinetic modeling analyses resulted in accurate estimates of lactate oxidation and metabolism. In contrast, supraphysiologic levels of plasma FFA (4,111 ± 1,709 nmol/mL) led to poor PET estimates of lactate metabolism due to negligible lactate oxidation (1% ± 2%) and complete backdiffusion of unmetabolized ^{11}C-lactate into the vasculature (28% ± 22%). **Conclusion:** Under conditions of net lactate extraction, L-3-^{11}C-lactate faithfully traces myocardial metabolism of exogenous lactate. Furthermore, in physiologic substrate environments, noninvasive measurements of lactate metabolism are feasible with PET using myocardial clearance analysis (oxidation) or compartmental modeling. Thus, L-3-^{11}C-lactate should prove quite useful in widening our understanding of the role that lactate oxidation plays in the heart and other tissues and organs.

Key Words: myocardial lactate oxidation; L-3-^{11}C-lactate; PET; kinetic modeling

J Nucl Med 2007; 48:2046–2055
DOI: 10.2967/jnumed.107.044503

Derangements in myocardial carbohydrate metabolism have been associated with impairment in cardiac function in diverse conditions ranging from normal aging (*1,2*) to diabetes mellitus (*3,4*), ischemic heart disease (*5*), and heart failure (*6*). Because of its inherent quantitative capabilities and diversity of metabolic radiotracers, PET has played a key role in characterizing perturbations in myocardial carbohydrate use associated with all of these conditions (*7–11*). To date, however, measurements of myocardial carbohydrate metabolism in humans have focused solely on glucose use because of the availability of excellent PET tracers of glucose uptake and metabolism such as ^{18}F-FDG (*8,10*) and 1-^{11}C-glucose (*7,9,11*).

As a key substrate for myocardial carbohydrate oxidation, lactate uptake and oxidation increases under a variety of conditions, including increases in cardiac work and plasma lactate levels (*12*). Moreover, alterations in lactate metabolism appear to play an important role in diabetic heart disease (*13*). Currently, measurements of myocardial lactate metabolism in humans are limited to invasive methods that require arterial (ART) and coronary sinus (CS) sampling due to the lack of a suitable PET lactate tracer.

In past years, the radiochemistry group in our institution was successful in labeling L-lactate in the third carbon (L-3-^{11}C-lactate) (*14*). For the purposes of modeling, the labeling of L-lactate on the C-3 position (L-3-^{11}C-lactate) is advantageous. For example, if lactate is labeled in the C-1 position, $^{11}CO_2$ will be released when pyruvate is converted to acetyl-CoA by pyruvate dehydrogenase. If lactate is labeled in the C-3 position, however, the labeled carbon is transferred to acetyl-CoA and is not released as $^{11}CO_2$ until after its entry and cycling in the tricarboxylic acid (TCA) cycle. Consequently, the slower turnover time for L-3-^{11}C-lactate in myocardium will potentially enhance

Received Jun. 26, 2007; revision accepted Sep. 11, 2007.
For correspondence contact: Pilar Herrero, ME, MS, Cardiovascular Imaging Laboratory, Edward Mallinckrodt Institute of Radiology, 510 S. Kingshighway Blvd., St. Louis, Missouri 63110.
E-mail: herrerop@mir.wustl.edu

our ability to measure the myocardial kinetics of the tracer. Accordingly, the purposes of the current study were (a) to determine how faithfully L-3-^{11}C-lactate traces myocardial lactate uptake and oxidation in vivo based on arterial and coronary sinus sampling and (b) to develop a compartmental model that would allow for noninvasive measurements of myocardial lactate use and oxidation by PET and L-3-^{11}C-lactate.

MATERIALS AND METHODS

Animal Preparation

All animal experiments were conducted in compliance with the Guidelines for the Care and Use of Research Animals established by Washington University's Animal Studies Committee. The purpose-bred 20- to 25-kg mongrel dogs were fasted, anesthetized, and instrumented as reported previously (*15,16*). Catheters were placed in the thoracic aorta via the femoral arteries for monitoring of arterial blood pressure and arterial sampling. One femoral vein was cannulated to obtain venous blood samples and to administer drugs. A coronary sinus catheter was placed via the right external jugular vein under fluoroscopic guidance as previously described (*15,16*).

To achieve a wide range in myocardial lactate uptake and oxidation, 23 dogs were studied under various interventions initiated 60–90 min before imaging (*15,16*). To enhance lactate uptake and oxidation, 5 dogs were studied during lactate infusion. Sodium L-(+)-lactate diluted in phosphate buffer (0.06 M NaH_2PO_4 and 0.0134 M Na_2HPO_4) was infused at a rate of 130 μmol/kg/min to increase plasma lactate concentration approximately 3–3.5 times over normal fasting levels (LACTATE). Further enhancement of lactate uptake and oxidation was achieved by concomitant administration of lactate and phenylephrine (0.84–1.6 μg/kg/min) in 7 dogs (LAC/PHEN). To increase lactate extraction and oxidation, 4 other dogs were studied during a hyperinsulinemic–euglycemic clamp, which entailed a continuous infusion of insulin (70 mU/kg/h) with an adjustable infusion of 20% dextrose (CLAMP). Finally, inhibition of lactate oxidation was attained in 7 dogs by infusion (1 mL/min) of 20% Intralipid ([IL] Fresenius Kabi Clayton, LP).

Imaging and ART/CS Sampling Protocol

All PET studies were performed on a Siemens ECAT 962 HR+. The electrocardiogram, arterial blood pressure, and heart rate were monitored throughout the study. A transmission scan was performed to correct for photon attenuation. To measure myocardial blood flow (MBF), ^{15}O-water (14.8 MBq/kg) was administered as an intravenous bolus and dynamic PET data were acquired for 5 min (5-s frames). After allowing for decay of ^{15}O radioactivity, 185–962 MBq of L-3-^{11}C-lactate (^{11}C-lactate) was administered as a bolus, followed by 60 min of dynamic data collection. To identify the ^{11}C-metabolites present in ART and CS blood samples, 50 μmol/kg of L-3-^{13}C-bolus (sodium salt; Cambridge Isotope Laboratories, Inc.) were injected into 8 dogs (2 IL, 1 CLAMP, 2 LACTATE, and 3 LAC/PHEN) immediately after the ^{11}C-lactate bolus injection. Simultaneous ART and CS blood samples were obtained at 5, 10, 15, 20, 25, 30, 45, and 60 min after ^{11}C- and ^{13}C-lactate administration for the measurement of ^{11}C-lactate, $^{11}CO_2$ (an indicator of lactate oxidation), ^{11}C-neutral, and ^{11}C-basic metabolites (*17*), as well as for measurements of ART ^{13}C-labeled lactate, pyruvate, glucose, and alanine. Paired ART/CS blood samples were also collected to determine blood gases, plasma substrates (glucose, free fatty acids [FFA], lactate), and insulin at baseline, before ^{11}C, and 30 and 60 min of imaging.

Radiochemical Synthesis

All the reagents were obtained from Sigma-Aldrich and used without further purification. The tracer L-3-^{11}C-lactate was synthesized using a modification of a 2-step enzymatic synthesis previously described (*18*). Briefly, a conical vial containing 3 mg of *N*-(diphenylmethylene) glycine *t*-butyl ester dissolved in 180 μL of acetonitrile/*N,N*-dimethylformamide and 4 μL of 5N KOH was used to trap the ^{11}C-methyl iodide (GE PETrace MeI Microlab). After 5 min of heating at 87°C, the reaction mixture was diluted with ethanol/acetonitrile and transferred to a conical flask containing 600 μL of 6N HCl, where it was hydrolyzed and taken to dryness at 150°C–170°C. The cooled contents were redissolved with 0.1 M Tris buffer, pH 8.5, and the enzymes and cofactors were premixed and added: α-ketoglutarate, pyridoxal-5-phosphate, flavin adenine dinucleotide, catalase, glutamic pyruvic transaminase, D-amino acid oxidase, and L-lactic dehydrogenase with β-nicotinamide adenine dinucleotide (reduced form). The mixture was incubated for 6–8 min at 50°C. The enzymes were heat-denatured and removed by passing the mixture through a cation-exchange resin cartridge, and the desired product was eluted with water. After adjusting the pH to 6–7 and filtering through a 0.22-μm filter, we obtained a sterile and pyrogen-free, clear, colorless solution ready for injection. The total radiochemical yield at end of synthesis (EOS) was 30%–45%. We consistently obtained from 555–1,480 MBq of product with a radiochemical purity of >95%, in a total synthesis time of 50 min that included the 12-min preparation of ^{11}C-methyl iodide. The product was found to be enzyme-free and contained <5 ppm total of nonradioactive lactic acid, in a 5-mL injectate. The enantiomeric purity was determined on a Chirex D-penicillamine specialty column (Phenomenex) and found it to be >98% as L-3-^{11}C-lactate.

Measurements of Unlabeled Plasma Substrates

Plasma glucose and lactate levels were assayed enzymatically with a 2300 STAT Plus Analyzer (YSI Life Sciences). Plasma FFA levels were measured using an enzymatic colorimetric method (NEFA C kit; Wako Chemicals USA). Plasma insulin was measured by radioimmunoassay (Linco Research Co.).

Measurements of Plasma ^{11}C-Lactate and its Metabolites

Plasma ^{11}C-lactate was separated from its metabolites by using a solid-phase approach (*17*). An anion-exchange resin (AG1-X4, 100–200 mesh, formate form; Bio-Rad) trapped the acidic metabolites (^{11}C-lactate and $^{11}CO_2$ as $NaH^{11}CO_3$). A cation-exchange resin (AG50W-X8, 200–400 mesh; Bio-Rad) trapped the basic metabolites with the neutral metabolites found in the final eluate. The $^{11}CO_2$ fraction in plasma was determined separately as previously described (*17*) and subtracted from total counts found on the acidic resin to obtain ^{11}C-lactate in plasma. With this approach, ^{11}C-lactate measurement probably also included some ^{11}C-pyruvate. On the other hand, the basic metabolites retained in the cation resin might include, besides alanine, other amino acids such as glutamate and glutamine, whereas the neutral fraction might include, besides glucose, some glycerol.

Measurement of Plasma ^{13}C-Lactate and Its Metabolites

Plasma ^{13}C-labeled lactate, pyruvate, and alanine enrichments were determined by gas chromatography mass spectrometry ([GC/

MS] 5973 MSD; Agilent Technologies) in a single run using tert-butyldimethylsilyl (TBDMS) or silylquinoxalinol TBDMS (for pyruvate) derivatives, monitoring ions at *m/z* 260 and 261 (for both lactate and alanine) or *m/z* 217 and 218 (for pyruvate). ^{13}C-Glucose enrichment was determined in a separate GC/MS run using the isopropylidine derivative, monitoring ions at *m/z* 287, 288, and 289 (to account for any doubly labeled glucose). Internal standards uniformly labeled with ^{13}C (e.g., U-^{13}C-lactate) were used to quantify the concentration of unlabeled substrate (e.g., lactate), which was then multiplied by the enrichment to derive the concentration of labeled substrate (e.g., 3-^{13}C-lactate).

PET Image Analysis and Measurement of MBF

Myocardial ^{15}O-water and ^{11}C-lactate images were reoriented to generate standard short-axis and long-axis views, and composite PET images of myocardial ^{15}O-water and ^{11}C-lactate were obtained. Blood and myocardial time–activity curves were then generated as previously described (*15,16*). MBF (mL/g/min) was quantified from blood and myocardial time–activity curve generated from myocardial PET images of ^{15}O-water using a compartmental modeling approach developed and validated previously by our group (*15,16*).

PET Measurements of Exogenous Lactate Metabolism

To assess whether oxidation of exogenous myocardial lactate could be measured noninvasively from PET myocardial clearance of ^{11}C-lactate, a monoexponential equation was fitted to the late clearance (starting at 20 min after tracer injection) of PET myocardial time–activity curves, and the estimated rate constants (k_{mono}, min^{-1}) were compared with $^{11}CO_2$ production measured from ART/CS blood samples using linear regression analysis. The estimated regression line was then used to convert k_{mono} values to fractional lactate oxidation. To further investigate whether exogenous lactate extraction, backdiffusion, and oxidation could be assessed with PET and ^{11}C-lactate, a 2-compartment kinetic model was implemented (Fig. 1). The model was based on direct ART/CS plasma measurements of ^{11}C-lactate and its metabolites in myocardium, which showed that once it is taken up by myocardium, ^{11}C-lactate is either oxidized or returned back to the vasculature (backdiffusion), with negligible conversion into ^{11}C-pyruvate and ^{11}C-alanine. Thus, the model configuration is based on the assumption that no tracer is retained by the myocardium (*19*).

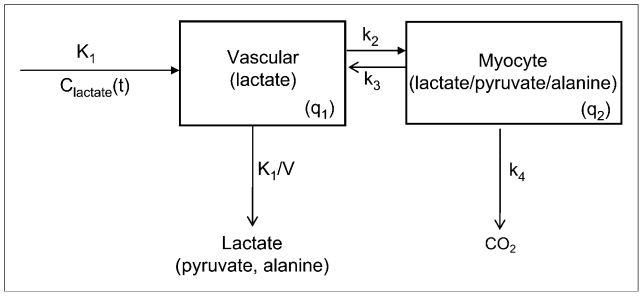

FIGURE 1. Kinetic model of exogenous L-3-^{11}C-lactate metabolism. $C_{lactate}(t)$ = arterial L-3-^{11}C-lactate activity over time (input function, cpm); K_1–k_4 = transfer rates; K_1 (mL/g/min) = vascular uptake; V (mL/g) = fractional myocardial vascular volume fixed to 0.08; K_1/V (min^{-1}) = vascular washout of tracer; k_2 (min^{-1}) = tracer transfer into nonvascular myocardium (myocyte); k_3 (min^{-1}) = backdiffusion of lactate and potential washout of metabolites (pyruvate, alanine); k_4 (min^{-1}) = lactate/pyruvate oxidation; q_n = myocardial tracer concentration in compartment n (counts/g).

The differential equations describing the modeling approach (Fig. 1) and the calculations of key rates of lactate metabolism are described below. The transport of tracer from one compartment to another can be described by the following differential equations:

$$dq_1/dt = K_1 \cdot C_{la}(t) - (K_1/V + k_2) \cdot q_1(t) + k_3 \cdot q_2(t), \quad \text{Eq. 1}$$

$$dq_2/dt = k_2 \cdot q_1(t) - (k_3 + k_4) \cdot q_2(t), \quad \text{Eq. 2}$$

where $C_{la}(t)$ is ^{11}C-lactate blood concentration (counts/mL) over time (input function), and q_n is the concentration of tracer in compartment n (counts/g). K_1 (mL/g/min) represents ^{11}C-lactate uptake into and washout from the vascular compartment, and k_2 (min^{-1}) represents the transfer of tracer from the vascular to the extravascular/cytosolic compartment, where ^{11}C-lactate is either back-diffused at a rate of k_3 (min^{-1}) or converted to pyruvate, transported into the mitochondrion, and oxidized at a rate of k_4 (min^{-1}).

Total tracer concentration in myocardium as a function of time was defined as the sum of tracer concentration in each compartment:

$$q_T(t) = \sum q_i(t),\ 1 \le i \le 2. \quad \text{Eq. 3}$$

Correction for partial-volume and spillover effects were accounted for within the model equation as previously described (*15,16*). Once model parameters were estimated using well-established numeric methods (*20,21*), $q_i(t)$ quantities were calculated as functions of rate constants by assuming the physiologic system is in steady state conditions—that is, differential equations are set to zero:

$$q_1 = (k_3 + k_4) \cdot q_2/k_2, \quad \text{Eq. 4}$$

$$q_2 = (K_1 \cdot k_2)/[(k_3 + k_4) \cdot (K_1/V + k_2) - k_2 \cdot k_3]. \quad \text{Eq. 5}$$

The following metabolic fluxes were then calculated from Equations 4 and 5.

$$\text{Lactate uptake (mL/g/min)} = k_2 \cdot q_1. \quad \text{Eq. 6}$$

$$\text{Lactate backdiffusion (mL/g/min)} = k_3 \cdot q_2. \quad \text{Eq. 7}$$

$$\text{Lactate oxidation (mL/g/min)} = (\text{Lactate uptake} - \text{Lactate backdiffusion}) = k_4 \cdot q_2. \quad \text{Eq. 8}$$

Myocardial fractional quantities were calculated from metabolic fluxes by dividing a given flux by MBF (mL/g/min). Measurements of the myocardial fate of lactate (use, backdiffusion, and oxidation, nmol/g/min) can be calculated as the product of plasma

lactate concentration (nmol/mL) and the corresponding flux (mL/g/min).

Statistical Analysis

All data are presented as mean ± SD. Comparisons between ^{11}C- and ^{13}C-metabolites were done by paired *t* test. Differences among interventions were compared by means of 1-way ANOVA, where the post hoc Fisher test was used to localize differences among groups. Correlations were calculated by linear regression analyses. A P value < 0.05 was considered statistically significant.

RESULTS

MBF and Oxygen Consumption

The heart rate ([HR] bpm) was not different among groups. The systolic blood pressure ([SBP] mm Hg), diastolic blood pressure ([DBP] mm Hg), and rate·pressure product ([RPP] mm Hg · bpm) did not differ among the 3 groups studied at rest (pooled mean values: 105 ± 16, 67 ± 13, and 9,026 ± 2,917, respectively) and were significantly higher during increased cardiac work (LAC/PHEN: 173 ± 34, 122 ± 21, and 14,542 ± 2,846, respectively, $P < 0.05$ vs. rested groups). Similarly, MBF (mL/g/min) and myocardial oxygen consumption ([MVO_2] μmol/g/min) were comparable among the 3 interventions performed at rest (0.75 ± 0.33 and 7.49 ± 4.45, respectively); and were significantly higher in LAC/PHEN (MBF: 1.41 ± 0.25, $P < 0.01$ vs. IL and LACTATE; MVO_2: 13.83 ± 3.95, $P < 0.05$ vs. IL, CLAMP, and LACTATE).

Plasma Substrates and Myocardial Substrate Use

By design, insulin levels were the highest in CLAMP ($P < 0.05$ vs. all groups), resulting in the highest myocardial glucose extraction and use in CLAMP ($P < 0.05$ vs. all groups). Plasma FFA levels were the highest in IL, resulting in the highest FFA use ($P < 0.05$ vs. all groups) (Table 1). Lactate infusion increased plasma lactate concentrations 4-fold above those in IL and CLAMP ($P < 0.05$). Comparable levels of plasma lactate in IL and CLAMP resulted in very different levels of lactate extraction with negligible extraction in IL and the highest among all groups in CLAMP ($P < 0.05$ vs. CLAMP, LAC/PHEN). Lactate use was the lowest in IL and the highest in LAC/PHEN ($P < 0.01$). Despite no differences in plasma insulin or substrate levels between LACTATE and LAC/PHEN, a 60% increase in cardiac work in LAC/PHEN (as measured by RPP) resulted in more than a doubling of myocardial lactate use (nmol/g/min) ($P < 0.05$), reflecting the combined effects of increased MBF and extraction of lactate.

Characterization of ^{11}C Acidic, Neutral, and Basic Metabolites

Figure 2 shows the time course of arterial ^{11}C acidic (A), neutral (B), and basic (C) metabolites and arterial ^{13}C-lactate + pyruvate (A), glucose (B), and alanine (C). As expected, ^{13}C-lactate metabolites (^{13}C-glucose and -alanine) appeared in arterial blood as lactate was removed from blood. The same pattern was observed for the ^{11}C neutral,

TABLE 1
Plasma Insulin and Substrate Arterial Concentration, Myocardial Extraction Fraction (EF), and Use

	Arterial concentration			Myocardial EF			Myocardial use			
Intervention	Insulin (μU/mL)	FFA (nmol/mL)	Glucose (μmol/mL)	Lactate (nmol/mL)	FFA	Glucose	Lactate	FFA (nmol/g/min)	Glucose (nmol/g/min)	Lactate (nmol/g/min)
IL ($n = 7$)	5.07 ± 3.43	4,111 ± 1,709*	5.48 ± 1.19	1,076 ± 398†	0.13 ± 0.10	−0.002 ± 0.030	0.083 ± 0.05‡§	261 ± 71*	−35 ± 74	67 ± 56§
CLAMP ($n = 4$)	94.62 ± 14.79*	146 ± 58	5.05 ± 0.55	1,009 ± 235†	0.45 ± 0.11*	0.23 ± 0.13*	0.38 ± 0.09	59 ± 43	662 ± 350*	307 ± 22§
LACTATE ($n = 5$)	2.36 ± 0.80	432 ± 152	5.82 ± 1.71	4,983 ± 1,130	0.13 ± 0.16	0.05 ± 0.09	0.19 ± 0.11‡	22 ± 25§	181 ± 320	609 ± 384§
LAC/PHEN ($n = 7$)	2.39 ± 1.35	556 ± 168	5.65 ± 0.28	4,320 ± 1,246	0.21 ± 0.12	0.01 ± 0.06	0.26 ± 0.06	137 ± 84	51 ± 103	1,388 ± 585

*$P < 0.05$ vs. all groups.
†$P < 0.05$ vs. LACTATE and LAC/PHEN.
‡$P < 0.05$ vs. CLAMP.
§$P < 0.01$ vs. LAC/PHEN.
IL = intralipid; CLAMP = hyperinsulinemic–euglycemic clamp; LAC = lactate; PHEN = phenylephrine; Myocardial EF = ([ART] – [CS])/[ART]; Myocardial use = ([ART] – [CS]) × MBF.
Values represent mean ± SD.

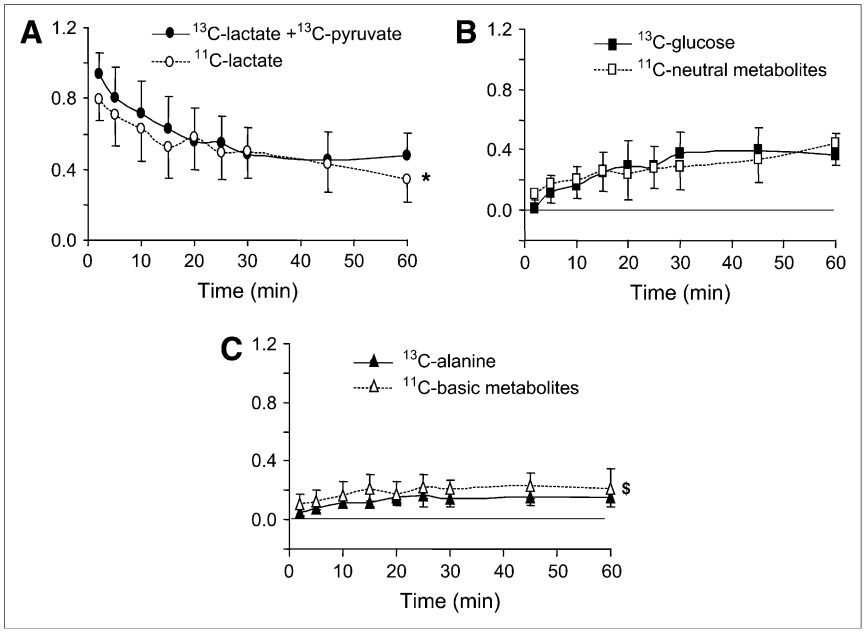

FIGURE 2. Time courses of fractional arterial ^{11}C activity (open symbols) for ^{11}C-lactate (A), ^{11}C-neutral (B), and ^{11}C-basic (C) metabolites and (solid symbols) for arterial ^{13}C-lactate + ^{13}C-pyruvate (A), ^{13}C-glucose (B), and ^{13}C-alanine (C). ^{11}C data represent fractions of total ^{11}C arterial activity, and ^{13}C data represent fractions of ^{13}C-(lactate + pyruvate + glucose + alanine). Graphs represent mean values for 8 dogs studied with ^{13}C-lactate ± SD. *$P < 0.05$ vs. ^{13}C-lactate + ^{13}C-pyruvate; $$P < 0.0001$ vs. ^{13}C-alanine.

basic, and acidic fractions. This close match between the time course of plasma ^{11}C and ^{13}C metabolites for lactate + pyruvate, glucose, and alanine strongly suggests the ^{11}C-lactate + pyruvate, ^{11}C-glucose, and ^{11}C-alanine are the primary labeled metabolites. However, a 45% ± 20% mean difference between the overall fractional contribution of ^{13}C-alanine and ^{11}C-basic fraction (0.12 ± 0.04 and 0.18 ± 0.05, respectively, $P < 0.0001$) is indicative of the presence of other basic metabolites such as glutamate and glutamine. In contrast, the contributions of ^{13}C-glucose and ^{11}C-neutral fraction to total arterial activity were no different (0.25 ± 13 and 0.26 ± 0.10, respectively, P = not significant). ^{13}C-Pyruvate isotopic enrichment was the same as that of ^{13}C-lactate 5-min after tracer injection, demonstrating that conversion of lactate to pyruvate occurred quite rapidly. Overall, 8% of the acidic fraction could be attributed to pyruvate, ranging from 5% in the CLAMP to 12% in LACTATE.

Accumulation of ^{11}C-lactate, $^{11}CO_2$, ^{11}C-neutral, and ^{11}C-basic metabolites over time in arterial blood for each intervention is shown in supplemental Figure S1 (supplemental Figures S1 and S2 are available online only at http://jnm.snmjournals.org). ^{11}C-Lactate decreased in all interventions over time, whereas $^{11}CO_2$ and ^{11}C-neutral metabolites increased and ^{11}C-basic metabolites remained unchanged. As expected, ^{11}C-lactate contribution was the highest in LACTATE and LAC/PHEN and the lowest in IL. The highest $^{11}CO_2$ contribution occurred in CLAMP. Thirty minutes after tracer injection, the contribution of ^{11}C-neutral metabolites to total ^{11}C arterial activity was greater than that of ^{11}C-lactate in IL, resulting in the highest contribution of ^{11}C-neutral metabolites to total arterial ^{11}C activity among all interventions. By 60 min, the contribution of ^{11}C-neutral metabolites to total arterial ^{11}C activity ranged from 23% to 28% in CLAMP, LACTATE, and LAC/PHEN to 45% in IL and was greater than the contribution of ^{11}C-basic metabolites, which overall contributed <11%. $^{11}CO_2$ contribution averaged 10%–13% in IL, LACTATE, and LAC/PHEN and 27% in CLAMP.

Myocardial extraction/production fractions obtained from ART and CS blood samples are shown in supplemental Figure S2. ^{11}C-Lactate extraction was not different from that of lactate in CLAMP and LACTATE and was significantly higher in LAC/PHEN at 60 min after tracer injection ($P < 0.05$). In contrast, during IL, ^{11}C-lactate plasma levels were higher in CS than in ART, resulting in an apparent net ^{11}C-lactate production ranging from 0.60 ± 0.14 at 5 min to 0.28 ± 0.22 at 60 min.

Thirty minutes after tracer injection, $^{11}CO_2$ production did not differ from lactate extraction in all non-Intralipid interventions, but was significantly lower than ^{11}C-lactate extraction at 60 min in LAC/PHEN ($P < 0.005$). During CLAMP, LACTATE, and LAC/PHEN, ^{11}C-neutral metabolites and ^{11}C-basic metabolites extractions were relatively low compared with lactate and ^{11}C-lactate extraction. In contrast, during IL, by 5 min after injection ^{11}C-neutral metabolites extraction was as high as lactate extraction and declined over time, whereas ^{11}C-basic metabolites were minimally produced during the entire study. In theory, the apparent net production of ^{11}C-lactate observed in IL could be attributed to either production of ^{11}C-lactate from ^{11}C-glucose or exogenous ^{11}C-lactate entering the myocyte and leaving it unchanged (backdiffusion). However, because the contribution of ^{11}C-glucose (^{11}C- neutral metabolites) to myocardial ^{11}C activity in IL was minimal (ranging from 0.046 ± 0.045 at 5 min to 0.01 ± 0.02 at 60 min), the apparent production of ^{11}C-lactate activity can be attributed only to ^{11}C-lactate backdiffusion.

A significant nonlinear correlation was observed between labeled and unlabeled lactate extractions (Fig. 3A), with apparent ^{11}C-lactate production in IL. It is apparent that the key contributor to the nonlinearity of the regression is the decline in extraction of ^{11}C-lactate in CLAMP as unlabeled lactate extraction increases, which could be attributed to the higher concentration of ^{11}C-lactate than unlabeled lactate in CS due to ^{11}C-lactate production from extracted ^{11}C-glucose (^{11}C-neutral metabolites in supplemental Fig. S2, CLAMP). In contrast, there was a strong linear correlation between $^{11}CO_2$ production and extraction of unlabeled lactate (Fig. 3B) with a slope not different from 1 ($r = 0.89$, $P < 0.0001$, slope = 1.20 ± 0.13). Because of the apparent production of ^{11}C-lactate in the IL group, a nonlinear correlation was observed between $^{11}CO_2$ production and ^{11}C-lactate extraction ($r = 0.80$, $P < 0.0001$). Removing the IL data resulted in significant linear correlation between $^{11}CO_2$ production and either unlabeled extraction ($r = 0.82$, $P < 0.0001$, slope = 1.14 ± 0.20) or ^{11}C-lactate extraction ($r = 0.58$ $P < 0.05$, slope = 0.68 ± 0.26), with a significantly higher slope observed with unlabeled extraction than ^{11}C-lactate extraction ($P < 0.05$).

PET Measurements of ^{11}C-Lactate Metabolism

Representative myocardial PET images of L-3-^{11}C-lactate early uptake (5–10 min after tracer injection) and the corresponding ^{11}C-time–activity curves are shown in Figure 4.

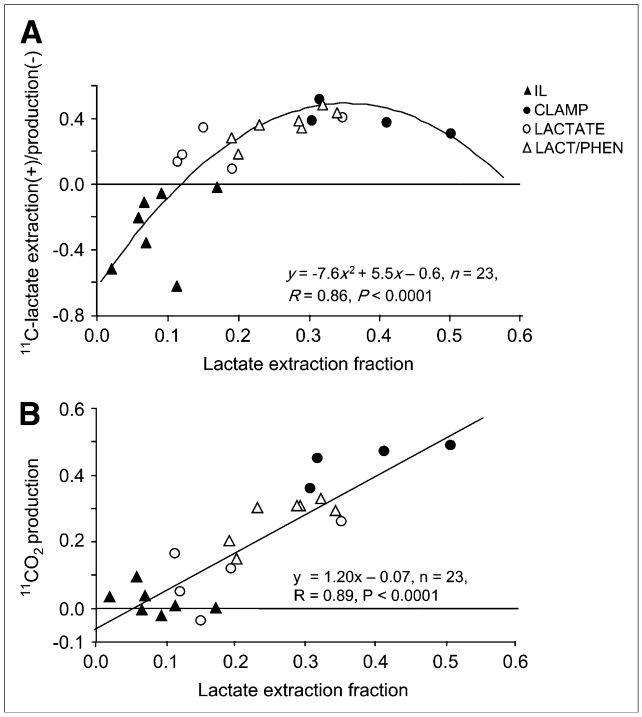

FIGURE 3. Correlation between ^{11}C-lactate extraction/production (*y*-axis, A) or $^{11}CO_2$ production (*y*-axis, B) and extraction fraction of unlabeled lactate (*x*-axis, A and B).

Tracer uptake was observed in all interventions with high lactate uptake (CLAMP: 0.38, LACTATE: 0.32, and LAC/PHEN: 0.28 mL/g/min) as well as in IL, where net lactate uptake was minimal (0.04 mL/g/min), corroborating the observations obtained from ART/CS blood samples, where severe suppression of myocardial ^{11}C-lactate oxidation in IL resulted in initial uptake before backdiffusion of unused tracer (supplemental Fig. S2). The early clearance of myocardial ^{11}C activity (Fig. 4A, solid dots, 1–20 min) with no apparent retention of tracer observed in the IL study is consistent with significant backdiffusion of tracer and negligible net lactate extraction and oxidation measured from the direct ART/CS measurements (supplemental Fig. S2). In the rest of the interventions (Figs. 4B–4D), myocardial time–activity curves displayed a plateau before clearance of tracer (5–10 min), indicative of significant tracer retention before it is removed from myocardium as ^{11}C-lactate (backdiffusion) or as $^{11}CO_2$.

Lactate oxidation estimated from PET clearance analysis correlated well with $^{11}CO_2$ production ($r = 0.80$, $P < 0.0001$), with the slope and intercept not different from 1 and 0, respectively. However, estimates of lactate oxidation were quite variable, especially in the IL study, where estimates ranged from −0.13 to 0.18 for a range in $^{11}CO_2$ production values between −0.003 and 0.039. After removing the IL study (Fig. 5A), a significant but weaker correlation was obtained ($r = 0.73$, $P < 0.001$), with the slope not different from 1 and the intercept not different from 0.

Excellent fits to the 4–rate-constant 2-compartment kinetic model were observed in all non-IL studies, resulting in good estimates of lactate oxidation (Fig. 5B) ($r = 0.81$, $P < 0.0005$). In IL, PET kinetics did not fit the model because severe inhibition of lactate oxidation resulted in almost complete backdiffusion of myocardial ^{11}C-lactate. This observation was corroborated by fitting PET kinetics to a simple 2–rate-constant, 1-compartment model describing exclusively uptake and washout of tracer. Excellent fits were obtained for all 7 IL studies.

Components of lactate metabolism estimated from kinetic modeling for nonintralipid studies are shown in Figure 5C. Initial tracer extraction and backdiffusion were the highest in LACTATE and CLAMP and the lowest in LAC/PHEN. Contribution of lactate oxidation to overall myocardial oxygen consumption (lactate oxidation/MVO_2) was the lowest in CLAMP where substrate competition was present, with no differences in lactate oxidation/MVO_2 between the LACTATE and LAC/PHEN.

DISCUSSION

To our knowledge, we have demonstrated for the first time that ^{11}C-lactate labeled in the third carbon follows the myocardial fate of exogenous lactate extraction, where it is either oxidized or backdiffused; with minimal myocardial

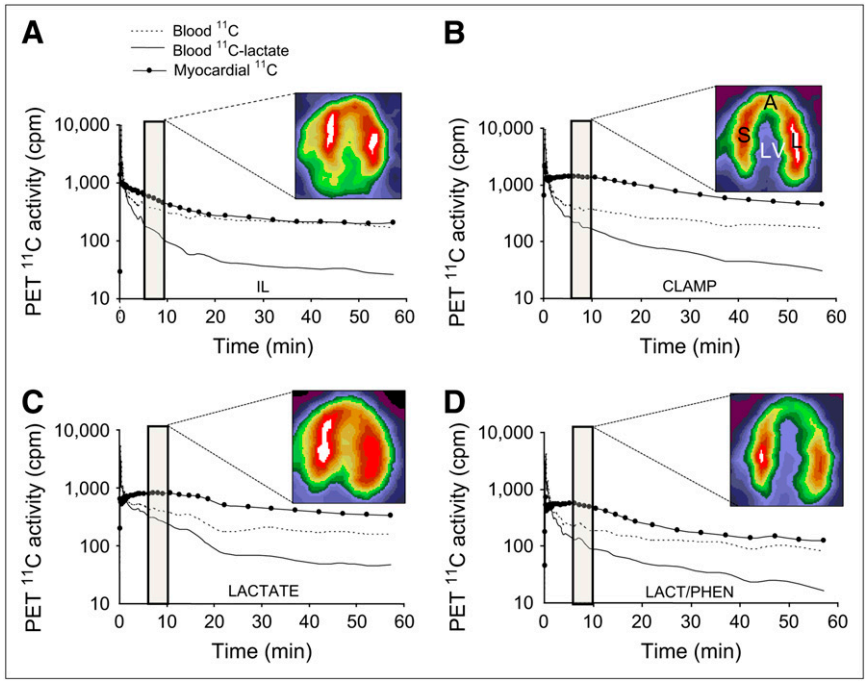

FIGURE 4. Representative PET time–activity curves of L-3-^{11}C-lactate obtained from IL, CLAMP, LACTATE, or LAC/PHEN studies and corresponding myocardial images obtained 5–10 min after tracer injection and depicting primarily early tracer uptake. Images are displayed on horizontal long axis. Blood ^{11}C = ^{11}C time–activity curves obtained from region of interest (ROI) placed on left atrium; blood ^{11}C-lactate = blood ^{11}C time–activity curves after removing $^{11}CO_2$, ^{11}C-neutral, and ^{11}C-basic metabolites; myocardial ^{11}C = ^{11}C time–activity curves obtained from ROI placed on lateral wall. A = apical wall; S = septal wall; L = lateral wall; LV = left ventricle.

contribution of secondarily labeled ^{11}C-glucose and ^{11}C-basic metabolites to myocardial ^{11}C activity. Furthermore, in interventions with physiologic FFA levels, myocardial PET clearance and kinetic modeling analyses resulted in good estimates of lactate oxidation (clearance analysis) and overall lactate metabolism, including initial uptake, backdiffusion and oxidation (kinetic model). In the presence of supraphysiologic levels of plasma FFA, both approaches failed due to severe inhibition of lactate oxidation resulting in very high levels of tracer backdiffusion.

Metabolism of L-3-^{11}C-Lactate: Direct Measurements

Arterial radiolabeled non-CO_2 acidic, neutral, and basic fractions obtained from ^{11}C-lactate represented lactate + pyruvate, glucose, and mostly alanine, respectively (Fig. 2). Eight percent of the acidic fraction could be attributed to pyruvate. Reported percentages measured in healthy individuals after an overnight fast averaged 16% (*22*). The most abundant ^{11}C fraction in arterial blood was lactate + pyruvate (43%), followed by neutral metabolites (glucose, 31%) and CO_2 (15%), with basic metabolites (primarily

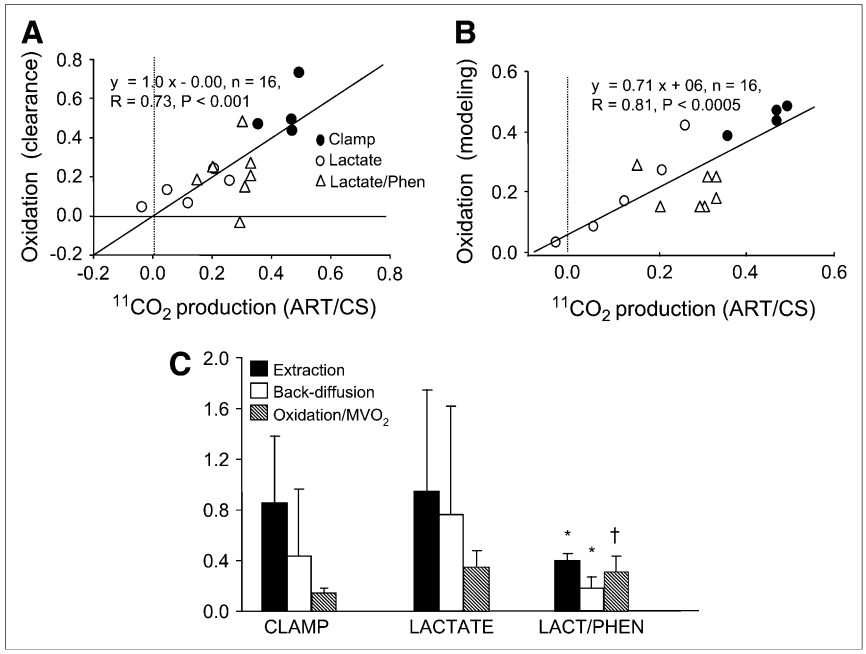

FIGURE 5. Correlation between PET measurements of fractional lactate oxidation and $^{11}CO_2$ production for all non-IL studies obtained from monoexponential clearance analysis of the late myocardial ^{11}C-lactate kinetics (20–60 min) (A) and from kinetic modeling (B). Initial lactate extraction, backdiffusion, and oxidation normalized by MVO_2 for non-IL studies estimated from compartmental modeling of ^{11}C-lactate PET kinetic (C). Bar graphs represent intervention mean ± SD. *P = 0.08 vs. extraction or backdiffusion in LACTATE; †P = 0.08 vs. oxidation/MVO_2 in CLAMP.

alanine) contributing 10% to total arterial ^{11}C activity (supplemental Fig. S1). The highest levels of arterial ^{11}C-glucose were observed in the IL study (45% of total ^{11}C activity vs. 26% in the non-IL interventions). The strong presence of ^{11}C-glucose in arterial blood is indicative of persistent gluconeogenesis from ^{11}C-lactate and consistent with enhanced gluconeogenesis in metabolic states with elevated plasma FFA levels, such as starvation and diabetes (*23*).

Despite the relatively high ^{11}C-glucose concentrations and the significant presence of ^{11}C-basic metabolites in plasma, ^{11}C-glucose was minimally extracted by the heart, with no significant extraction of ^{11}C-basic metabolites (supplemental Fig. S2), suggesting that, under the conditions studied, secondarily labeled ^{11}C-lactate metabolites undergo minimal myocardial extraction and, therefore, should not interfere with noninvasive myocardial PET measurements of exogenous ^{11}C-lactate metabolism. These observations contrast with our recent study on measurements of glucose metabolism using 1-^{11}C-glucose, where myocardial contribution of secondarily labeled ^{11}C-lactate produced from 1-^{11}C-glucose was significant and had to be considered to accurately measure myocardial glucose metabolism beyond its initial uptake (*24*).

Myocardial ^{11}C-lactate extraction was higher than that of unlabeled lactate in all non-IL interventions, resulting in $^{11}CO_2$ production greater than lactate extraction (Fig. 3B). These results are consistent with results of earlier studies in humans using arteriovenous measurements of 1-^{14}C-lactate and L-U-^{13}C-lactate (*19,25*). Greater myocardial extraction of tracer than unlabeled lactate was observed in these studies because of the simultaneous release of unlabeled lactate produced from glycolysis of unlabeled glucose. In a subsequent study (*12*) it was observed that the underestimation of true lactate extraction by measuring net lactate extraction also resulted in levels of exogenous lactate oxidation that, even though correlated well with net lactate extraction, were significantly higher than net lactate extraction.

In the presence of supraphysiologic plasma FFA levels and low lactate extraction, apparent production of ^{11}C-lactate could not be attributed to production of ^{11}C-lactate from glycolysis of secondarily labeled ^{11}C-glucose, as minimal myocardial extraction of ^{11}C-glucose was observed in all interventions (supplemental Fig. S2). However, the positive correlation between plasma FFA levels and ^{11}C-lactate production observed in IL ($r = 0.75$, $P < 0.05$) strongly suggests that this apparent production of lactate represents unoxidized myocardial ^{11}C-lactate that diffuses back into the vasculature due to severe inhibition of ^{11}C-lactate oxidation in the presence of high levels of acetyl-CoA derived from FFA oxidation (*26,27*). These observations clearly demonstrate that the primary fate of myocardial ^{11}C-lactate originating from exogenous ^{11}C-lactate is either oxidation or backdiffusion. These assumptions are consistent with earlier observations in humans where oxidation of exogenous lactate accounted for practically all extracted 1-^{14}C-lactate (99.5%) as measured by $NaH^{14}CO_3$ production in which all ^{14}Cs contributing to $^{14}CO_2$ were trapped (*19*).

In the present study, changes in ^{11}C-lactate oxidation among interventions as measured by $^{11}CO_2$ production were consistent with expected changes in lactate oxidation due to insulin, substrate, and cardiac work changes. For instance, severe inhibition of ^{11}C-lactate oxidation was observed in the IL study, where supraphysiologic plasma FFA levels resulted in negligible lactate oxidation (supplemental Fig. S1, 60 min). On the other hand, the highest levels of lactate oxidation were observed in CLAMP (supplemental Fig. S2, 60 min), where low plasma levels of FFA due to inhibition of lipolysis by insulin, and the subsequent low FFA uptake and oxidation, resulted in enhanced lactate oxidation. These observations are in keeping with what is known about the regulation of pyruvate oxidation in the heart. Pyruvate oxidation is primarily regulated by FFA at the level of acetyl-CoA, where high levels of acetyl-CoA generated from FFA oxidation result in inhibition of carbohydrate oxidation by the pyruvate dehydrogenase complex (PDH). Conversely, low levels of acetyl-CoA from FFA oxidation activate the PDH complex, resulting in enhancement of glucose and lactate oxidation (*26–31*).

In the 2 interventions with supralactate plasma levels, increase in cardiac work, as demonstrated by the doubling of the RPP, resulted in a 2-fold increased in lactate oxidation. These observations are consistent with the well-known role of lactate during cardiac work, where it becomes a key myocardial respiratory substrate by increasing oxidation proportionally to cardiac work (*6,32,33*). Thus, it appears evident that ^{11}C labeling of L-lactate in the third carbon position (L-3-^{11}C-lactate) results in an excellent tracer of myocardial lactate metabolism.

Metabolism of L-3-^{11}C-Lactate: PET Measurements

Currently, noninvasive measurements of myocardial lactate metabolism are not possible because of the lack of tracers or methodologies to be used in conjunction with difference images modalities such as magnetic resonance spectroscopy and PET. To evaluate whether noninvasive measurements of exogenous lactate metabolism could be attained using PET, 2 different methodologies were used: monoexponential analysis of myocardial PET ^{11}C-clearance (oxidation only) and kinetic modeling (lactate metabolism).

The strong correlation observed between lactate oxidation obtained from PET measurements of myocardial ^{11}C clearance rates (k_{mono}) and $^{11}CO_2$ production (Fig. 5A) clearly shows that good indices of lactate oxidation can be obtained noninvasively with ^{11}C-lactate and PET using a simple clearance approach. However, as mentioned previously, the accuracy of the method declines markedly under conditions of excessive backdiffusion of intact tracer, such as under conditions of very low lactate oxidation.

Although indices of lactate oxidation can be quite useful, the strength of PET lies in its capacity for noninvasive and quantitative measurements of physiologic processes. The PET kinetic model implemented was based on the understanding of the myocardial fate of exogenous ^{11}C-lactate obtained from ART/CS measurements in which tracer taken into myocardium is either oxidized or back-diffuses into the vasculature (Fig. 1). These observations are consistent with measurements of lactate oxidation in humans (*19*), where it accounted for practically all extracted 1-^{14}C-lactate (99.5%) as measured by $NaH^{14}CO_3$ production, in which all ^{14}Cs contributing to $^{14}CO_2$ were trapped.

In this first attempt to model exogenous lactate metabolism, it was assumed that there were no detectable differences between $^{11}CO_2$ produced from carboxylation or decarboxylation. However, some of the underestimation in lactate oxidation observed in the LAC/PHEN study (Fig. 5B) might suggest otherwise, as during high cardiac work, faster depletion of the TCA cycle would result in increasing anaplerosis and, consequently, an increased contribution of anaplerotic $^{11}CO_2$ to total lactate oxidation. Not surprisingly, modeling resulted in better estimates of lactate oxidation where clearance of tracer in myocardium is defined by 3 distinct washout rates—vascular lactate, myocyte lactate, and lactate oxidation (Fig. 1)—whereas clearance analysis allowed only for 2 washout rates.

Significance of Lactate Oxidation Measurements Using L-3-^{11}C-Lactate

In spite of the well-known fact that the heart uses a wide range of substrates, including FFA, glucose, lactate, and, to a lesser extent, pyruvate and ketone bodies, the great majority of cardiac substrate metabolism studies traditionally have concentrated on glucose and FFA use. This is most probably due, as has been proposed by others (*34*), to the misperception that lactate is a minor fuel when compared with glucose and FFA. On the contrary, results of studies in isolated perfuse hearts, intact animals, and humans have demonstrated that lactate oxidation is a major cardiac fuel, contributing significantly to carbohydrate oxidation during cardiac work and elevated plasma lactate levels (*12*) with diminished contribution in ischemia and diabetes (*5,13*). To date, the lack of noninvasive lactate radiotracers has hampered our understanding of the critical role that lactate oxidation plays in the metabolic homeostasis of the heart and, consequently, the development of potential metabolic therapies designed to restore cardiac function by normalizing cardiac substrate metabolism. Thus, access to a novel noninvasive tracer should prove quite useful in widening our understanding of the role that lactate oxidation plays in the heart and other tissues and organs.

CONCLUSION

Under conditions of net lactate extraction, L-3-^{11}C-lactate traces myocardial metabolism of exogenous lactate faithfully. Moreover, under physiologic conditions of net lactate extraction, it is feasible to measure myocardial lactate metabolism using L-3-^{11}C-lactate in conjunction with PET and kinetic modeling. Use of PET and L-3-^{11}C-lactate should allow for the noninvasive measurements of myocardial lactate metabolism, thus permitting a more complete assessment of myocardial carbohydrate metabolism in physiologic as well as clinical studies.

ACKNOWLEDGMENTS

This study was supported by NIH grants HL-69100 and grant HL-13851. We thank Nerissa Torrey, Margaret Morris, and Shalonda W. Scott for their technical assistance.

REFERENCES

1. Kates AM, Herrero P, Dence C, et al. Impact of aging on substrate metabolism by the human heart. *J Am Coll Cardiol.* 2003;41:293–299.
2. Aasum E, Hafstad AD, Severson DL, Larsen TS. Age-dependent changes in metabolism, contractile function, and ischemic sensitivity in hearts from db/db mice. *Diabetes.* 2003;52:434–441.
3. Meigs JB, Singer DE, Sullivan LM, et al. Metabolic control and prevalent cardiovascular disease in non-insulin-dependent diabetes mellitus (NIDDM): The NIDDM Patient Outcome Research Team. *Am J Med.* 1997;102:38–47.
4. Mahgoub MA, Abd-Elfattah AS. Diabetes mellitus and cardiac function. *Mol Cell Biochem.* 1998;180:59–64.
5. Stanley WC, Lopaschuk GD, Hall JL, et al. Regulation of myocardial carbohydrate metabolism under normal and ischaemic conditions: potential for pharmacological interventions. *Cardiovasc Res.* 1997;33:243–257.
6. Stanley WC, Recchia FA, Lopaschuk GD. Myocardial substrate metabolism in the normal and failing heart. *Physiol Rev.* 2005;85:1093–1129.
7. Soto PF, Herrero P, Kates AM, et al. Impact of aging on myocardial metabolic response to dobutamine. *Am J Physiol Heart Circ Physiol.* 2003;285:H2158–H2164.
8. Hällsten K, Virtanen KA, Lönnqvist F, et al. Enhancement of insulin-stimulated myocardial glucose uptake in patients with type 2 diabetes treated with rosiglitazone. *Diabet Med.* 2004;21:1280–1287.
9. Herrero P, Peterson LR, McGill JB, et al. Increased myocardial fatty acid metabolism in patients with type 1 diabetes mellitus. *J Am Coll Cardiol.* 2006;47:598–604.
10. Hernandez-Pampaloni M, Bax JJ, Morita K, Dutka DP, Camici PG. Incidence of stunned, hibernating and scarred myocardium in ischaemic cardiomyopathy. *Eur J Nucl Med Mol Imaging.* 2005;32:314–321.
11. Dávila-Román VG, Vedala G, Herrero P, et al. Altered myocardial fatty acid and glucose metabolism in idiopathic dilated cardiomyopathy. *J Am Coll Cardiol.* 2002;40:271–277.
12. Gertz EW, Wisneski JA, Stanley WC, Neese RA. Myocardial substrate utilization during exercise in humans: dual carbon-labeled carbohydrate isotope experiments. *J Clin Invest.* 1988;82:2017–2025.
13. Wang P, Lloyd SG, Zeng H, Bonen A, Chatham JC. Impact of altered substrate utilization on cardiac function in isolated hearts from Zucker diabetic fatty rats. *Am J Physiol Heart Circ Physiol.* 2005;288:H2102–H2110.
14. Dence CS, Lee H, Kim J-K, Sun X, Laforest R, Welch MJ. Synthesis, microPET imaging biodistribution and dosimetry data of D- and L-3-^{11}C lactic acid [abstract]. *J Labelled Comp Radiopharm.* 2003;46(suppl):S-97.
15. Herrero P, Weinheimer CJ, Dence C, Oellerich WF, Gropler RJ. Quantification of myocardial glucose utilization by PET and 1-carbon-11-glucose. *J Nucl Cardiol.* 2002;9:5–14.
16. Herrero P, Sharp TL, Dence C, Haraden BM, Gropler RJ. Comparison of 1-^{11}C-glucose and ^{18}F-FDG for quantifying myocardial glucose use with PET. *J Nucl Med.* 2002;43:1530–1541.
17. Dence CS, Herrero P, Schwarz SW, Mach RH, Gropler RJ, Welch MJ. Imaging myocardium enzymatic pathways with carbon-11 radiotracers. In: Abelson JN, Simon MI, eds. *Methods in Enzymology.* Vol. 385. Pasadena, CA: Elsevier Academic Press; 2004:286–315.
18. Bjurling P, Långström B. Synthesis of 1- and 3-^{11}C labeled L-lactic acid using multi-enzyme catalysis. *J Labelled Comp Radiopharm.* 1990;28:427–432.

19. Gertz EW, Wisneski JA, Neese R, Bristow JD, Searle GL, Hanlon JT. Myocardial lactate metabolism: evidence of lactate release during net chemical extraction in man. *Circulation.* 1981;63:1273–1279.
20. Gear CW. *Numerical Initial-Value Problems in Ordinary Differential Equations*. Englewood Cliffs, NJ: Prentice-Hall; 1971.
21. Dennis JE, Schnabel RB. *Numerical Methods for Unconstrained Optimization and Nonlinear Differential Equations*. Englewood Cliffs, NJ: Prentice-Hall; 1983.
22. Rasmussen P, Plomgaars P, Krogh-Madsen R, et al. MCA Vmean and arterial lactate-to-pyruvate ratio correlate during rhythmic handgrip. *J Appl Physiol.* 2006; 101:1406–1411.
23. Boden G, She P, Mozzoli M, et al. Free fatty acids produce insulin resistance and activate the proinflamatory nuclear factor-κB pathway in rat liver. *Diabetes.* 2005;54:3458–3465.
24. Herrero P, Kisrieva-Ware Z, Dence CS, et al. PET measurements of myocardial glucose metabolism with 1-^{11}C-glucose and kinetic modeling. *J Nucl Med.* 2007; 48:955–964.
25. Wisneski JA, Gertz EW, Neese RA, Gruenke LD, Morris DL, Craig JC. Metabolic fate of extracted glucose in normal human myocardium. *J Clin Invest.* 1985;76:1819–1827.
26. Schonekess BO. Competition between lactate and fatty acids as sources of ATP in the isolated working heart. *J Mol Cell Cardiol.* 1997;29:2725–2733.
27. Bartelds B, Knoester H, Beaufort-Krol GCM, et al. Myocardial lactate metabolism in fetal and newborn lambs. *Circulation.* 1999;99:1892–1987.
28. Randle PJ. Fuel selection in animals. *Biochem Soc Trans.* 1986;14:799–806.
29. Hansford RG, Cohen L. Relative importance of pyruvate dehydrogenase interconversion and feed-back inhibition in the effect of fatty acids on pyruvate oxidation by rat heart mitochondria. *Arch Biochem Biophys.* 1978;191:65–81.
30. Ferrannini E, Santoro D, Bonadonna R, Natali A, Parodi O, Camici PG. Metabolic and hemodynamic effects of insulin on human hearts. *Am J Physiol.* 1993;264:E308–E315.
31. McNulty PH. Comparison of local and systemic effects of insulin on myocardial glucose extraction in ischemic heart disease. *Am J Physiol Heart Circ Physiol.* 2000;278:H741–H747.
32. Goodwin GW, Taylor CS, Taegtmeyer H. Regulation of energy metabolism of the heart during acute increase in heart work. *J Biol Chem.* 1998;273:29530–29539.
33. Beaufort-Krol GCM, Takens J, Molenkamp C, et al. Increased myocardial lactate oxidation in lambs with aortopulmonary shunts at rest and during exercise. *Am J Physiol.* 1998;275:H1503–H1512.
34. Chatham JC. Lactate: the forgotten fuel! *J Physiol.* 2002;542:333.